Temperature dependence of the dielectric tensor of monoclinic Ga_2O_3 single crystals in the spectral range 1.0–8.5 eV

C. Sturm, R. Schmidt-Grund, V. Zviagin, and M. Grundmann

Citation: Appl. Phys. Lett. **111**, 082102 (2017); doi: 10.1063/1.4999763

View online: https://doi.org/10.1063/1.4999763

View Table of Contents: http://aip.scitation.org/toc/apl/111/8

Published by the American Institute of Physics

Temperature dependence of the dielectric tensor of monoclinic Ga_2O_3 single crystals in the spectral range 1.0–8.5 eV

C. Sturm, R. Schmidt-Grund, V. Zviagin, and M. Grundmann
Felix-Bloch-Institut für Festkörperphysik, Universität Leipzig, Linnéstr. 5, 04103 Leipzig, Germany

(Received 4 May 2017; accepted 4 August 2017; published online 21 August 2017)

The full dielectric tensor of monoclinic Ga_2O_3 (β-phase) was determined by generalized spectroscopic ellipsometry in the spectral range from 1.0 eV up to 8.5 eV and temperatures in the range from 10 K up to 300 K. By using the oriented dipole approach, the energies and broadenings of the excitonic transitions are determined as a function of the temperature, and the exciton-phonon coupling properties are deduced. *Published by AIP Publishing*. [http://dx.doi.org/10.1063/1.4999763]

The large bandgap energy of about 4.8 eV[1–3] makes Ga_2O_3 interesting as a transparent conductive oxide (TCO) material since even in the presence of impurities, e.g., caused by doping, a high transmissivity is sustained in the visible and even in the UV-A/B spectral range. At ambient conditions, Ga_2O_3 exhibits a monoclinic crystal structure in the thermodynamic equilibrium, the so-called β-phase. Its dielectric function (DF) is a tensor consisting of four independent quantities. The knowledge of the magnitude and the dispersion of all four tensor elements are important for the interpretation of the optical response, e.g., the Raman spectrum,[4,5] and for the design of optoelectronic devices since it allows to deduce the optical anisotropic properties, such as the presence and orientation of optic and singular axes.[3,6] However, the determination of the full dielectric tensor requires a series of polarization sensitive measurements and thus cannot be obtained by standard reflectivity and absorption measurements which are typically carried out on bulk single crystals.[1,2,7,8] Recently, the full dielectric tensor of β-Ga_2O_3 was determined by generalized spectroscopic ellipsometry at room temperature from the infared[6,9] up to the UV spectral range.[3,6]

Here, we report on the temperature dependence of the full dielectric tensor in the temperature range of 10–300 K in the spectral range of 1.0–8.5 eV by generalized spectroscopic ellipsometry. By means of a line shape analysis, the properties of the excitonic transitions as a function of the temperature and the exciton-phonon coupling properties are deduced and discussed.

We investigated two commercial bulk single crystals with $(\bar{2}01)$ and (010) surface orientations by generalized ellipsometry. The samples and the experimental details are described in Ref. 3. Note that for the investigations presented in this work, the samples were mounted on a liquid helium flow cryostat, and thus, the available in-plane rotation angles were limited to 0° and 90°, whereas the angle of incidence is limited to 70°. The impact of the cryostat windows on the Mueller matrix elements was calibrated by using a Si reference sample and verified by measuring the Ga_2O_3 samples at room temperature with and without the cryostat. For the line shape analysis of the experimental data, we used a model dielectric function which takes oriented dipole transitions into account.[6] Within this model, the components of the dielectric tensor are defined by the projection of the polarization of these dipoles, oscillating along directions defined by the non-orthogonal crystal symmetry, into the laboratory system. By using this approach, all components of the dielectric tensor are Kramers-Kronig consistent. Details on this approach as well as the contributions of the model dielectric function and the layer stack model are given in Ref. 6. Since for the monoclinic crystal structure, no well-defined directions in the *a*-*c*-plane exist to define a Cartesian coordinate system, we chose the dielectric system with directions given by $\tilde{e}_x \parallel a$-axis, $\tilde{e}_y \parallel b$-axis, and $\tilde{e}_z = \tilde{e}_x \times \tilde{e}_y$ with $\tilde{e}_i$ being the unit vector in the *i*-direction, and "$\times$" the vector cross product. Within this coordinate system, the dielectric tensor is given by

$$\epsilon = \begin{pmatrix} \epsilon_{xx} & 0 & \epsilon_{xz} \\ 0 & \epsilon_{yy} & 0 \\ \epsilon_{xz} & 0 & \epsilon_{zz} \end{pmatrix}. \quad (1)$$

In order to describe the optical response of the samples and the experimental spectra, the dielectric tensor was transferred for each in-plane orientation from the dielectric system into the laboratory system by means of the Euler angles.[10]

The experimentally determined and calculated Mueller matrix (MM) elements are in good agreement with each other for all orientations and temperatures as exemplarily demonstrated in Fig. 1(a) for a selected crystal orientation for $T = 10$ K and 300 K. The remaining minor deviations at high energies can be attributed to the limitations of the effective medium approach used for the surface layer. In the investigated temperature range, the MM does not show a strong change in the observed features. This is also reflected by the deduced components of the DF [Fig. 1(b)]. Its temperature dependent change can be mainly attributed to a red shift of the transition peak energies with increasing temperature. A strong enhancement or narrowing of these peaks for low temperatures, as it is the case for conventional III-V or II-VI semiconductors like GaAs[11] and GaN,[12] is not observable. This indicates that the oscillator strength and the broadening of the transitions are almost temperature independent.

In the investigated spectral range, the DF is dominated by excitonic polarizabilities, and thus, the observed peaks in the DF can be attributed to excitonic transitions.[3,13] The contribution of these transitions to the DF was described by a model function developed by Tanguy[14–16] which takes into account

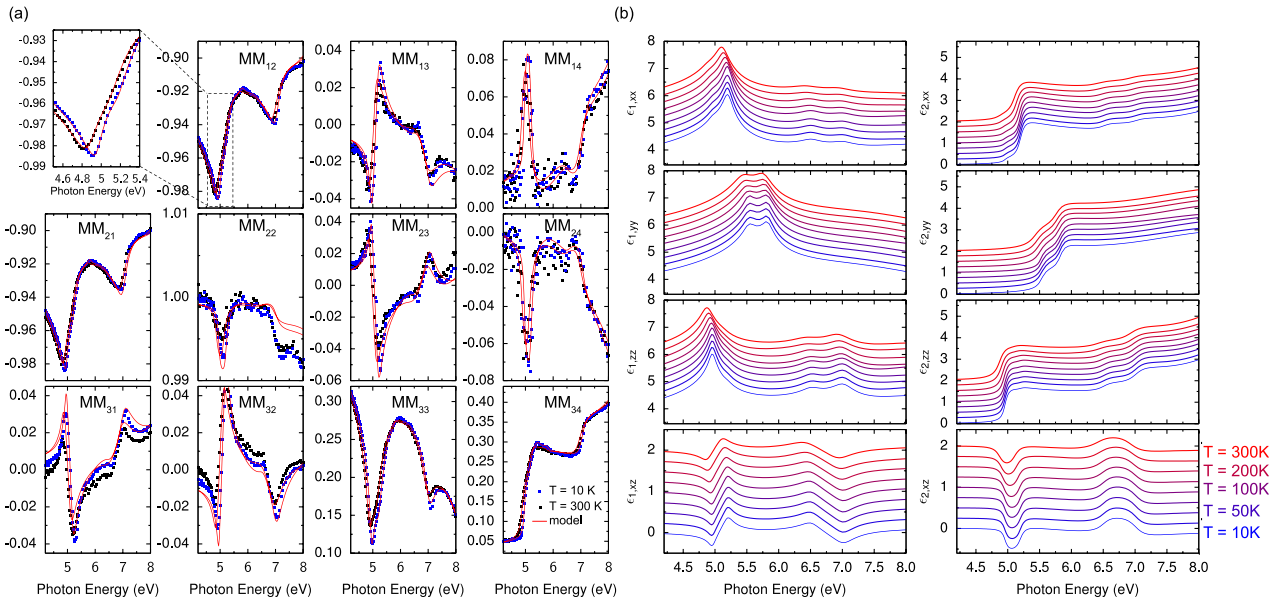

FIG. 1. (a) Experimental (symbols) and calculated (lines) Mueller matrix spectra in the absorption spectral range of a (010)-oriented β-Ga_2O_3 bulk single crystal exemplarily for 10 K and 300 K as indicated. The crystallographic *a*-axis is perpendicular to the plane of incidence, whereas the *b*-axis is parallel to the surface normal. The MM was calculated by means of model C (see text). Note that the shown experimental and calculated Mueller matrix spectra include also the phase shift caused by the windows of the used cryostat. (b) Components of the dielectric tensor as a function of temperature. The functions were shifted vertically with respect to each other for a better clarity.

their broadening, the energy of the fundamental bound state, the exciton binding energy, and the screening factor of the Coulomb potential. The current discussion will be limited to the temperature dependent properties of the excitonic transitions in the investigated spectral range. Further information regarding the used model dielectric function, the dipole orientation, and the involved orbitals of the excitonic transitions are given in Refs. 6 and 13. Note that in the experiments performed here, the sensitivity to the exciton binding energy, the dipole orientation of the excitons, and the screening factor are reduced as compared to the measurements performed at room temperature due to the limited availability of in-plane orientations and angles of incidence. Therefore, we fixed these quantities for all temperatures to those determined previously at room temperature, i.e., the binding energy and screening factor are set to $E_X^b = 270$ meV and $S = 0.7$, respectively.[6]

For the determination of the exciton ground state energy as a function of temperature, we used three models. In model A, all energies were determined independently of each other and for each temperature. In order to reduce correlation effects occurring in model A, in models B and C, we make use of the fact that the exciton energy is related to the bandgap energy by the exciton binding energy. Therefore, its change as a function of temperature can be attributed to the change in the lattice constants and the increasing interaction with lattice vibrations (phonons) towards higher temperatures. Both effects can be described by a Bose-Einstein model presented by Viña *et al.*[17]

$$E(T) = E_0 - \frac{\alpha E_p}{\exp\left(E_p/k_B T\right) - 1}. \qquad (2)$$

Here, E_0, α, and E_p represent the zero temperature transition energy, the exciton-phonon coupling strength, and the averaged energy of the phonons which are involved in the exciton-phonon coupling, respectively. The absence of narrow spectral features in the experimental data causes strong correlation between the parameters of the Bose-Einstein model. In order to reduce this correlation, we assume in model B the same average phonon energy for the respective transitions polarized in one plane or rather direction, i.e., $E_{p,x-z}$ and $E_{p,y}$ for the transitions polarized within the *x*–*z*-plane and along the *y*-axis, respectively. In contrast to that, in model C, E_p was assumed to be the same for all transitions independently of their polarization direction. Note that the mean squared error (MSE) for these three models is similar and ranges from 4.19 to 4.27.

The resulting change in the exciton energy obtained by the Tanguy line shape analysis as a function of the temperature is shown in Fig. 2(a), yielding a good agreement of all models. Model B yields for the electrons related to the transitions polarized within the *x*–*z*-plane an average energy of the phonons which are involved in the electron-phonon coupling of about $E_p = 50 \pm 5$ meV. This energy agrees very well with the barycenter of the phonon density of states calculated by using *ab-initio* and density function theory.[18,19] The corresponding coupling strength was determined to be $\alpha = 10.5 \pm 0.5$. For the transitions polarized along the *y*-axis, we obtain a smaller phonon energy and coupling strength of about $E_p = 25 \pm 3$ meV and $\alpha = 5.5 \pm 1.5$, respectively. A comparison to the calculated phonon density of states indicates that mainly phonons related to Ga atoms couple to these transitions. We bear in mind that the weakly pronounced transitions in the experimental data and the related uncertainty of the determined transition energies at elevated temperatures might also be responsible for the difference in the electron-phonon coupling properties for the two polarizations. Thus, in model C, we assume the same phonon energy for all transitions. In this case, we obtain a phonon energy of about $E_p = 58 \pm 5$ meV and a coupling strength of $\alpha = 13 \pm 1$ which is in good agreement with those determined

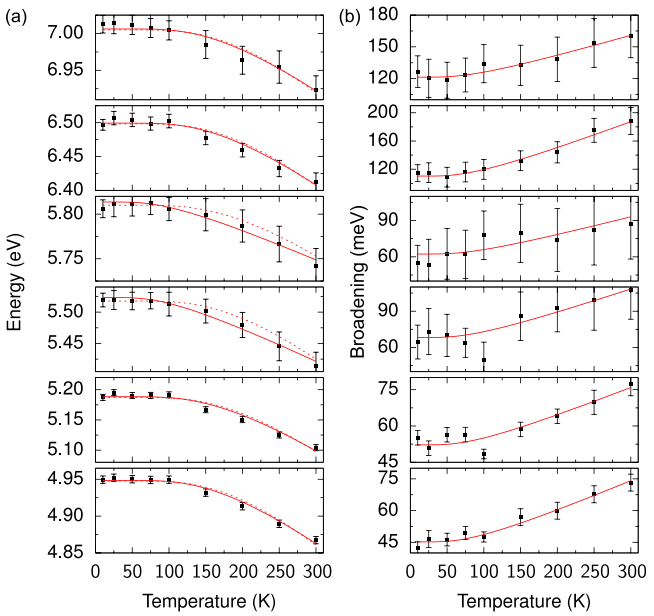

FIG. 2. (a) Exciton ground state energy as a function of temperature. The symbols represent the energies which were determined independently of each other (model A), whereas the red solid and dashed lines represents the energy determined by means of the Bose-Einstein model, assuming the same phonon energy for the transitions polarized in one plane (model B) and for all transitions (model C), respectively. (b) Broadening of the excitonic transitions. The symbols and red solid lines represent the broadening extracted from the line shape analysis and the best match taking into account exciton-LO-phonon coupling, respectively.

previously for the transitions polarized within the x–z-plane. The obtained electron-phonon coupling strength is about 2 … 5 times larger than that determined in other wide bandgap oxide semiconductors like ZnO ($\alpha \approx 2$)[20] and In_2O_3 ($\alpha \approx 3 \ldots 6$).[21]

The determined broadening of all excitonic transitions as a function of temperature is shown in Fig. 2(b). As expected, we observe an increase with the increasing temperature which can be attributed to a dephasing of the excitons caused by the interaction with acoustic and longitudinal optical (LO) phonons. In order to describe the observed change of the broadening with increasing temperature, we used a Bose-Einstein model[17]

$$\Gamma(T) = \Gamma_0 + \frac{\beta E_{\mathrm{p}}^{\mathrm{g}}}{\exp\left(E_{\mathrm{p}}^{\mathrm{g}}/k_B T\right) - 1}, \tag{3}$$

with Γ_0, β, and $E_{\mathrm{p}}^{\mathrm{g}}$ being the zero temperature broadening, the exciton-phonon coupling strength, and the averaged energy of the involved phonons, respectively. In order to reduce the correlation between the involved parameters, corroborated by the findings of the temperature dependence of the exciton energies, we assume the same average phonon energy for all transitions. Thus, the zero temperature broadening and the exciton-phonon coupling strength depend only on the transition energy. The best match between the experimental and calculated data is shown in Fig. 2(b) as red solid lines, resulting in an average phonon energy of $E_{\mathrm{p}}^{\mathrm{g}} \approx 21$ meV. This energy is smaller than the average phonon energy ruling the shift of the transition energies.

The determined broadening and the exciton-phonon coupling strength is shown in Fig. 3 as a function of the

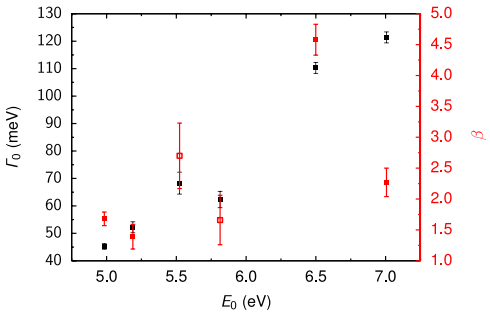

FIG. 3. The extracted zero temperature broadening (black symbols) and the exciton-LO-phonon coupling strength (red symbols) of the excitonic transitions as a function of the zero temperature transition energy. The filled and open symbols represent the transition polarized within the x-z-plane and along the y-direction, respectively.

zero temperature exciton transition energy. We observe an increase in the zero temperature broadening with increasing transition energy from $\Gamma_0 \approx 45$ meV up to $\Gamma_0 \approx 120$ meV. Interestingly, the obtained data reveal that the increase in the broadening is independent of the polarization and orientation of the involved transitions. An increase in the zero temperature broadening was also observed for semiconductors like Ge,[17] GaAs,[11] and ZnO.[20] For the exciton-photon coupling strength, there might also be an increase with increasing transition energy. For the energetically lowest excitons, the determined coupling strength is smaller than in other wide bandgap oxide semiconductors like ZnO ($\beta \approx 6$)[22] and In_2O_3 ($\beta \approx 4$).[21]

A relevant material property, especially for applications, is the refractive index or rather DF in the transparent spectral range. However, due to the non-vanishing off-diagonal elements, the simple relationship $n_i = \sqrt{\epsilon_i}$ between the components of the refractive index (n_i) and the dielectric tensor does not hold, and thus, we limit the discussion to the DF. In this spectral range ($E \leq 3.7$ eV), the DF is real-valued and can be described by a Cauchy-like line shape function.[3] We found that in this spectral range, the tensor elements depend linearly on the temperature for a given energy, and thus, the DF as a function of the temperature can be expressed as

$$\epsilon_{1,ij} = A_{0,ij} + A_{T,ij}T + \frac{B_{0,ij} + B_{T,ij}T}{\lambda^2} + \frac{C_{0,ij} + C_{T,ij}T}{\lambda^4} \tag{4}$$

and $\epsilon_{1,xy} = \epsilon_{1,yz} = 0$. The index 0 represents the zero temperature coefficients, whereas the temperature dependence is given by the coefficients with the index T. The corresponding parameters are listed in Table I.

TABLE I. Parameters of the tensor elements of the dielectric function of β-Ga_2O_3 in the spectral range (1.0 eV $\leq E \leq$ 3.7 eV). The uncertainty is given by the last digit.

		ϵ_{xx}	ϵ_{yy}	ϵ_{zz}	ϵ_{xz}
A_0		3.49	3.62	3.57	0.01
B_0	(10^{-2} μm^2)	3.78	3.76	3.91	–0.01
C_0	(10^{-3} μm^4)	2.09	1.76	2.45	–0.21
A_{T}	(10^{-5} K^{-1})	8.04	6.20	2.01	0.86
B_{T}	(10^{-6} μm^2 K^{-1})	1.91	2.35	–0.61	0.02
C_{T}	(10^{-7} μm^4 K^{-1})	6.12	3.76	7.36	–0.92

To summarize, we determined the temperature dependence of the full dielectric tensor for temperatures from $T = 10\,\mathrm{K}$ to $T = 300\,\mathrm{K}$. The determined change of the exciton transition energy yields an electron-phonon coupling strength of about $\alpha = 10.5 \pm 0.5$ and an average phonon energy of $E_p = 58 \pm 5\,\mathrm{meV}$, which agrees quite well with the barycenter of the phonon density of states. This indicates that all phonons affect the electronic band structure. The analysis of the exciton broadening as a function of temperature demonstrated an increase in the zero temperature broadening with increasing transition energy.

This work was supported by the Deutsche Forschungsgemeinschaft within Sonderforschungsbereich 762-"Functionality of Oxide Interfaces" and we are grateful for fruitful discussions within Leibniz ScienceCampus GraFOx.

[1]N. Ueda, H. Hosono, R. Waseda, and H. Kawazoe, Appl. Phys. Lett. **71**, 933 (1997).
[2]M. Yamaga, T. Ishikawa, M. Yoshida, T. Hasegawa, E. G. Villora, and K. Shimamura, Phys. Status Solidi C **8**, 2621 (2011).
[3]C. Sturm, J. Furthmüller, F. Bechstedt, R. Schmidt-Grund, and M. Grundmann, APL Mater. **3**, 106106 (2015).
[4]C. Kranert, C. Sturm, R. Schmidt-Grund, and M. Grundmann, Sci. Rep. **6**, 35964 (2016).
[5]C. Kranert, C. Sturm, R. Schmidt-Grund, and M. Grundmann, Phys. Rev. Lett. **116**, 127401 (2016).
[6]C. Sturm, R. Schmidt-Grund, C. Kranert, J. Furthmüller, F. Bechstedt, and M. Grundmann, Phys. Rev. B **94**, 035148 (2016).
[7]T. Matsumoto, M. Aoki, A. Kinoshita, and T. Aono, Jpn. J. Appl. Phys., Part 1 **13**, 1578 (1974).
[8]Z. Galazka, R. Uecker, K. Irmscher, M. Albrecht, D. Klimm, M. Pietsch, M. Brützam, R. Bertram, S. Ganschow, and R. Fornari, Cryst. Res. Technol. **45**, 1229 (2010).
[9]M. Schubert, R. Korlacki, S. Knight, T. Hofmann, S. Schöche, V. Darakchieva, E. Janzén, B. Monemar, D. Gogova, Q.-T. Thieu, R. Togashi, H. Murakami, Y. Kumagai, K. Goto, A. Kuramata, S. Yamakoshi, and M. Higashiwaki, Phys. Rev. B **93**, 125209 (2016).
[10]H. Goldstein, C. P. Poole, and J. Safko, *Classical Mechanics*, 3rd ed. (Pearson Education, 2011).
[11]P. Lautenschlager, M. Garriga, S. Logothetidis, and M. Cardona, Phys. Rev. B **35**, 9174 (1987).
[12]S. Logothetidis, J. Petalas, M. Cardona, and T. D. Moustakas, Phys. Rev. B **50**, 18017 (1994).
[13]J. Furthmüller and F. Bechstedt, Phys. Rev. B **93**, 115204 (2016).
[14]C. Tanguy, Phys. Rev. Lett. **75**, 4090 (1995).
[15]C. Tanguy, Phys. Rev. Lett. **76**, 716 (1996).
[16]C. Tanguy, Phys. Rev. B **60**, 10660 (1999).
[17]L. Viña, S. Logothetidis, and M. Cardona, Phys. Rev. B **30**, 1979 (1984).
[18]B. Liu, M. Gu, and X. Liu, Appl. Phys. Lett. **91**, 172102 (2007).
[19]S. Yoshioka, H. Hayashi, A. Kuwabara, F. Oba, K. Matsunaga, and I. Tanaka, J. Phys.: Condens. Matter **19**, 346211 (2007).
[20]T. Makino, C. H. Chia, N. T. Tuan, Y. Segawa, M. Kawasaki, A. Ohtomo, K. Tamura, and H. Koinuma, Appl. Phys. Lett. **76**, 3549 (2000).
[21]R. Schmidt-Grund, H. Krauß, C. Kranert, M. Bonholzer, and M. Grundmann, Appl. Phys. Lett. **105**, 111906 (2014).
[22]R. Schmidt-Grund, N. Ashkenov, M. M. Schubert, W. Czakai, D. Faltermeier, G. Benndorf, H. Hochmuth, M. Lorenz, and M. Grundmann, AIP Conf. Proc. **893**, 271 (2007).